Data Acquisition and Quality Analysis of 3-Dimensional Fingerprints

Yongchang Wang, Qi Hao, *Member, IEEE*, Abhishika Fatehpuria,
Laurence G. Hassebrook, *Senior Member, IEEE*, and Daniel L. Lau, *Member, IEEE*

Abstract

This paper introduces a new technology of non-contact 3D fingerprint capture and processing for higher quality fingerprint data acquisition. The system relies on a real-time 3D sensor using structured light illumination (SLI), which generates both texture and detailed ridge depth information. The high resolution 3D scans are then converted into 2D flat equivalent fingerprints. As a result, many limitations imposed upon conventional fingerprint capture and processing can be reduced by the unobtrusiveness of this approach and the extra depth information acquired. The image quality of 2D flat equivalent fingerprint is evaluated and analyzed using NIST fingerprint image software. A comparison is performed between the unraveled 3D fingerprints and their 2D plain counterparts in terms of fingerprint quality.

I. INTRODUCTION

Fingerprint recognition has been extensively applied in both forensic law enforcement and security applications involving personal identification [1]–[3]. Traditional fingerprint acquisition is performed in 2D using contact methods which have evolved over the last century, from ink (rolled or plain) to capacitive, ultrasonic, pyroelectric, thermal, and optoelectronic approaches [4]–[7]. Among fingerprint capture approaches, contact based devices detect the geometric difference between contact and non-contact parts (i.e. ridges and valleys) of the finger on the device. The optical approach, on the other hand, captures the texture information of the fingerprint under examination.

A typical automatic fingerprint identification system (AFIS) consists of four modules: image acquisition, preprocessing, feature extraction, and feature matching [8], [9]. In the image acquisition, a digital image of the fingerprint is captured from either an inked fingerprint impression, or electronic signals of a fingerprint sensor, or a live scan of the finger. The preprocessing module assesses the quality of an acquired fingerprint and further enhances the acquired image for feature extraction. Specific features are then extracted to represent the image in a certain feature space to facilitate matching. The matching module computes the likelihood of the extracted feature set matching with a template feature set. The performance of the system depends on how well each module performs and higher matching performance will be achieved if fingerprint quality is sufficiently high.

In many applications that require high precision fingerprints, limitations are imposed upon the current fingerprint capture technologies [10], [11], including:

1) obligatory maintenance of a clean sensor or prism surface;
2) uncontrollability and non-uniformity of the finger pressure on the device;
3) permanent or semi-permanent change of the finger ridge structure due to injuries or heavy manual labors;
4) residues from the previous fingerprint capture;
5) data distortion under different illumination, environmental, and finger skin conditions; and
6) extra scanning time and motion artifacts incurred in technologies that require finger rolling.

The majority of these limitations arise due to the physical contact of the finger surface with the sensor plate, or the nonlinear distortion introduced by the 3D-to-2D mapping during image acquisition [12]. Besides the robust operation, an ideal AFIS system also requires automatic fingerprint entry, high-speed data acquisition, real-time feedback, and low cost. To address these issues, several novel technologies have been developed [13]–[16] that avoid direct contact between the sensor and the skin.

In [15], [16], Parziale *et al* proposed multi-camera touchless fingerprint scanner which acquires different finger views that are combined together to provide a 3D representation of the fingerprint. Due to the lack of contact between the elastic skin of the finger and any rigid surface, the acquired images preserve the fingerprints "ground-truth" without skin deformation during acquisition [16]. However, employing the shape-from-silhouette scanning technique, the ridge information is obtained from the surface reflection variation (i.e. albedo) information. Thus, the fingerprint is sensitive to surface color, surface reflectance, geometric factors and some other effects.

We have been developing a non-contact 3D scanning system that employs structured light illumination (SLI). Our ultimate goal is to simultaneously acquire 3D scans of all the five fingers and the palm in high speed and fidelity using multiple, commodity digital cameras and a DLP projector. Post processing of these scans is then performed to virtually extract the finger and palm surfaces, and create 2D flat equivalent images.

This work is partially funded by Flashscan3D, LLC, Richardson, TX and National Institute of Hometown Security, Somerset, KY.

The authors are with the Center for Visualization and Virtual Environments, University of Kentucky, Lexington, KY 40507. Qi Hao is now with the Electrical and Computer Engineering Department of The University of Alabama. Laurence G. Hassebrook is a member of Flashscan3D, LLC. ywang6@engr.uky.edu, qh@eng.ua.edu, abhishika@uky.edu, lgh@engr.uky.edu, dllau@engr.uky.edu

Fig. 1. Prototype scanner for 3D fingerprint scanning.

The advantages of the presented 3D fingerprint scanning and processing technology include:

1) non-contact defuses distortion that exists in conventional fingerprint acquisition system.
2) simultaneous acquisition of both texture and ridge depth information of fingers;
3) automated fingerprint entry in no need of interaction with the operator;
4) fast scanning (less than 1 second);
5) robustness to contamination of fingers and residues of previous users;
6) robustness to clutter and fraud because of the difficulties in faking 3D fingerprints;
7) real-time feedback (less than 5 seconds) for users to make position adjustment; and
8) low cost by using the off-the-shelf commodity camera and projector.

The rest of this paper is organized as follows. Section II describes the 3D acquisition setup. Section III presents the methods to convert 3D scans to 2D flat equivalent finger images. Section IV describes the fingerprint quality evaluation methods. Section V presents the experimental results. Section VI outlines future works.

II. Data Acquisition

The system under study relies on 3D image acquisition through a SLI approach. The sensor was developed by Flashscan3D LLC. and the University of Kentucky. Fig. 1 shows the prototype 3D fingerprint scanner. Fig. 2 shows the a 3D fingerprint obtained by the prototype scanner. The algorithm for fingerprint scanning is phase measuring profilometry (PMP) [17]–[20]. PMP originates from the classical optical interferometry techniques.

Compared to other structure light algorithms like single spot, light stripe and gray code projection, the PMP technique uses fewer patterns for a given precision [20], [21]. PMP projects shifted sine wave patterns and captures a deformed fringe pattern for each shift. The projected light pattern is expressed as [18], [20]

$$I_n^p(x^p, y^p) = A^p + B^p cos(\phi(x^p, y^p) + 2\pi n/N), \tag{1}$$

where (x^p, y^p) are the projector coordinates, A^p and B^p are projector constants, the subscript n represents the pattern index, N is the total number of patterns, and $\phi(x^p, y^p)$ is the phase of the sine wave which is assigned as:

$$\phi(x^p, y^p) = 2\pi f \frac{y^p}{L}, \tag{2}$$

where f is the frequency of the sine wave, and L is the length of the sine wave (length or height of the resolution of projector) [18], [20].

From the camera viewpoint, the captured image is distorted by the object topology in terms of [18], [20]

$$I_n^c(x^c, y^c) = A^c(x^c, y^c) + B^c(x^c, y^c) cos[\phi(x^c, y^c) - \frac{2\pi n}{N}], \tag{3}$$

where $I_n^c(x^c, y^c)$ represents the intensity of n^{th} pattern at pixel location (x^c, y^c) of the captured image, A^c and B^c are the albedo and modulation information, and $\phi(x^c, y^c)$ represents the phase value at pixel location (x^c, y^c) of the captured sine wave pattern. Thus, $\phi(x^c, y^c)$ can be computed from the captured images as follows [18], [20]

$$\phi(x^c, y^c) = arctan \left[\frac{\sum_{n=1}^{N} I_n^c(x^c, y^c) sin(2\pi n/N)}{\sum_{n=1}^{N} I_n^c(x^c, y^c) cos(2\pi n/N)} \right]. \tag{4}$$

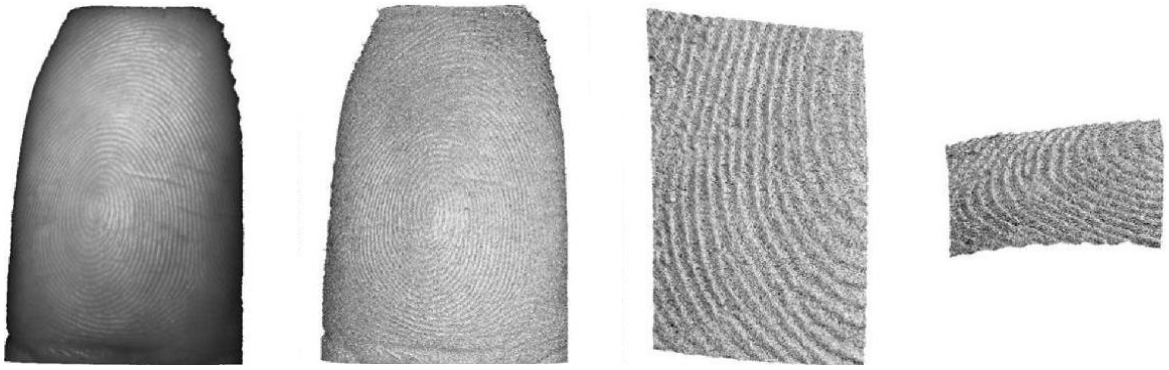

(a) (b) (c) (d)

Fig. 2. A 3D fingerprint scan. (a) A 3D finger with texture (surface reflectance variations or albedo image). (b) 3D fingerprint with depth rendering. (c) Cropped 3D fingerprint with depth rendering. (d) Rotated crop.

As the phase value can only be estimated between $[-\pi, \pi]$, the value of projector coordinate is between $[-1/2f, 1/2f]$, which will limit the measurable depth range of objects. A total of $N = 10$ phase shift patterns with frequency $f = 16$ cycles/field of view is chosen to make a trade-off between scanning time and resolution.

Once the value of $\phi(x^c, y^c)$ is obtained, the projector coordinate y^p of a 3D point with a camera coordinate (x^c, y^c) can be recovered from [18], [20]

$$y^p(x^c, y^c) = \phi(x^c, y^c)\frac{L}{2\pi f}. \tag{5}$$

Based on the matched camera and projector coordinates $(x^c, y^c, y^p(x^c, y^c))$, the 3D depth can be computed using the perspective projection matrix obtained through a joint projector and camera calibration [18]–[20].

III. 3D Data Processing

There are two ways to develop an AFIS system using 3D fingerprints: (1) 3D image based and (2) 2D flat equivalent image based. The former requires to develop new feature extraction and matching methods. The latter can make use of the existing algorithms for 2D fingerprint processing, after 3D fingerprint scans are unraveled into 2D flat equivalent fingerprints. The 2D flat equivalent fingerprints are further processed to be compliant with the National Institute of Standard and Technology (NIST) standards. The process of pressing an inked finger on a paper sheet or on a platen is, inherently, a 3D process as the acquired print is dependent on the fingerprint ridge depth variation. In fact, 3D fingerprint scan acquisition provides a digital analogy to this cumbersome analog process.

We have developed an algorithm to unravel 3D scans into 2D equivalent images using a similar idea. The best fit tube algorithm is developed from the spring algorithm [22] and best fit sphere algorithm [23]. Generally speaking, the algorithm finds the best fit tube to the fingerprint surface. The original 3D data is then unraveled by flattening the tube. The ridge information of the fingerprint is extracted from the unraveled 3D surface. Ridge depth is converted to gray level. The gray level unraveled 3D fingerprint contains the similar ridge information as in 2D inked fingerprint as well as other information like pores on the finger and height of ridges. After binarization, the 2D depth flattened fingerprint is down-sampled to the required points per inch (PPI) resolution according to Criminal Justice Information Services (CJIS) specifications.

Noting that albedo image is also available in 3D data, we can obtain the ridge information from the albedo image as well, and fuse the fingerprints obtained out of both albedo and depth data. The fusion is based on a local quality map produced by NIST software. The fused fingerprint has a higher quality than either the albedo or the depth unraveled image alone. The outer scan rim of the finger is outside the focal depth of the camera lens. As such, the 3D fingerprint is cropped down the region out of focus.

Figure 3 shows a contrast between a 2D plain fingerprint image obtained from Cogent CSD450 and a 2D equivalent image unraveled from 3D data. It can be seen that: 1) for most parts, ridges are clear in both 2D plain and unraveled 3D fingerprints; 2) the 2D plain fingerprint has a small empty area in the top-right part due to its larger color variation; 3) ridges in the unraveled 3D fingerprint are more equally spaced which indicates less distortion in 3D data; and 4) there are several concave scars in the fingerprint where 3D uncovers more ridge information than 2D plain.

IV. Fingerprint Quality Performance

An automatic fingerprint recognition system can perform well on ideal fingerprint images with clear ridges and valleys. However, various skin conditions or imperfect acquisitions make the captured fingerprint image far from ideal. Also, unclean sensor plates, as well as, non-uniform and inconsistent contact can result in poor samples and, hence, increase false acceptance/rejection rates. Fingerprint matching involves computing the likelihood of the fingerprint coming from

(a) (b) (c)

Fig. 3. The fingerprint scan. (a) A 2D plain fingerprint. (b) The corresponding 3D scan. (c) The 2D unraveled equivalent obtained from 3D scan.

subjects in the database. Higher matching performance can be achieved if a fingerprint's quality is sufficiently good. It is, hence, desirable to assess the quality of a fingerprint before any matching process.

Many biometric literatures have addressed the problem of assessing fingerprint image quality [24]–[26]. It quantifies the local orientation information, global uniformity and continuity, amplitude and variance of spectral bases, or effective feature number of fingerprint images. In addition to removing the poor quality or invalid input images, fingerprint image quality can also be used as a predictor of matcher performance before a matching algorithm is applied [27].

For this 3D fingerprint study, as large public databases have not been available to test its matching performance, it is specifically important to evaluate the fingerprint scanner performance in terms of those fingerprint image quality matrices. And since the 3D fingerprints are unraveled to 2D equivalent fingerprints, the NIST Fingerprint Image Software (NFIS) for traditional 2D fingerprints becomes applicable to those 2D equivalent fingerprints for the purpose of evaluating the 3D fingerprint scanner.

The NFIS is a public domain source code distribution including several packages for fingerprint quality purpose: [27]:

1) PCASYS: pattern classification system,
2) MINDTCT: minutiae detection system,
3) NFIQ: fingerprint image quality system,

The PCASYS system is a prototype classifier that separates the fingerprints into basic pattern-level classes such as *arch, left loop, right loop, scar, tented arch,* or *whorl* based on the position of the singular components like the core, the delta and the direction of the ridge flow. Along with the fingerprint class, PCASYS also outputs an estimated posterior probability of the hypothesized class, which is a measure of the confidence that may be assigned to the classifier's decision. The confidence level generated for the hypothesis, is the probability value $(1 - \alpha)$, associated with the confidence interval, where α is the level of significance. A good quality image running through the PCASYS system will generate a high confidence level, closer to 1, in its corresponding class.

MINDTCT takes a fingerprint image and locates all minutiae in the image, assigning to each minutia point its location, orientation, type, and quality. The minutiae quality is assessed based on local image conditions and the orientation of each minutiae in addition to their location and type. To locally analyze the image, MINDTCT divides the image into a grid of blocks and assesses the quality of each block (4 being the highest quality and 0 being the lowest) [27]. The background has a score of 0. The percentage of blocks with quality 1, 2, 3, and 4 are calculated and are regarded as quality zones 1, 2, 3, and 4 respectively. Fingerprints with higher quality zone number of 4 are more desirable.

The MINDTCT software also computes quality or reliability measures to be associated with each detected minutiae point based on two factors. A quality value in the range from 0.01 to 0.99 is assigned to each minutiae, where a low quality minutiae number represents minutiae detected in low quality regions of the image whereas a high quality minutiae value indicates minutiae detected in the higher quality regions. Minutiae with quality number less than 0.5 are considered unreliable, while a quality number greater than 0.75 are considered to be highly reliable [27]. The better the image quality, more will be the number of reliable minutiae detected.

NFIQ measures the quality of a fingerprint image sample in two steps. First, it computes a multi-dimensional feature vector, which contains certain characteristics of the sample. Then it computes a non-linear mapping from the feature vector to the sample [27]. Those feature vectors are used in a matching algorithm. The image quality is determined from the feature vector using a neural network. NFIQ classifies the fingerprint images into 5 classes wherein a quality number 1 represents excellent quality and 5 poor quality. The quality number information is a useful quantitative metric because the information provided by the quality number can be used to determine low quality samples, helping improve scanning technology.

All the aforementioned statistics, including the confidence level, the number of reliable minutiae, local quality zone

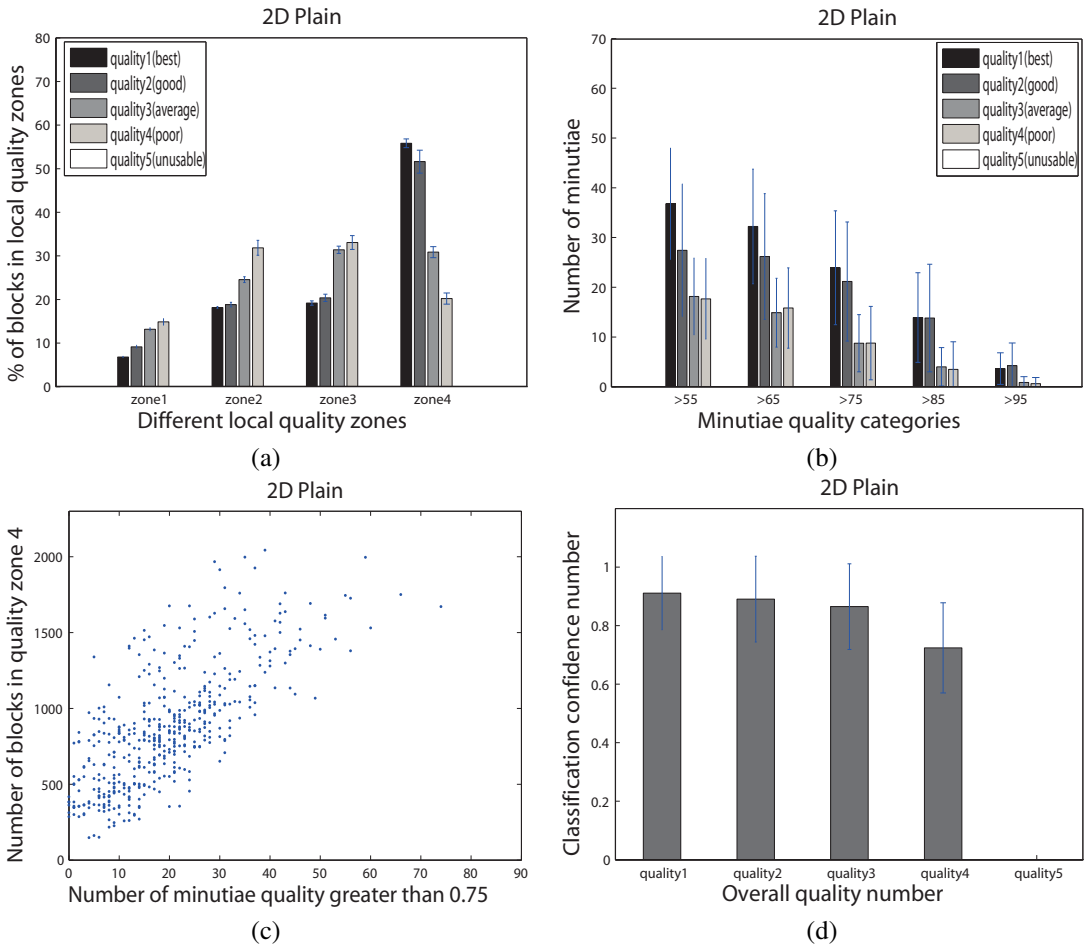

Fig. 4. Performance analysis for 2D plain fingerprint images. Quality 1 is the best overall quality of the fingerprints. (a) Distributions of informative blocks over local quality zones (1∼4) for images with different overall qualities. Zone4 represents the highest local quality. (b) Distributions of minutiae over minutiae quality numbers greater than 0.55, 0.65, 0.75, 0.85 and 0.95 for 2D plain fingerprints with different overall image qualities. (c) Scatter plot between the number of blocks with the best local quality and the number of minutiae with reliability greater than 0.75. (d) Plot of classification confidence numbers with respect to overall image quality numbers.

number and overall quality number, can help us evaluate the quality of the fingerprints obtained from a 3D scanner and the performance of the 3D scanner, before performing a computationally expensive matching evaluation upon a large 3D fingerprint database [27].

V. Experimental Results and Discussions

In this study, we develop some quantitative measures for evaluating the performance of the presented 3D fingerprint scanning and processing. We use statistical metrics including overall image quality, local image quality, minutiae quality, and classification confidence number, to perform scanner evaluation, we also collected the conventional 2D plain fingerprints using Cogent CSD450 from the same group of subjects. The evaluation results with NIST software from both sets of data were compared. A superior scanning technology should generate a higher confidence number on classification, a higher number of reliable minutiae (greater than 20), more blocks with high local quality (zone4 representing the highest local quality), and a lower overall image quality number (1 representing the highest overall quality).

A 3D fingerprint database was created for this purpose at the University of Kentucky. The database contains both 2D plain fingerprint images and unraveled fingerprints of 3D scans from 11 subjects, 441 fingerprints in each category. All ten fingers of each subject were scanned by using the SLI prototype scanner described in section II. The 3D scans were unraveled into 2D equivalent images, and processed with the NIST programs. The corresponding 2D plain images were processed by the same procedure as comparison.

Each fingerprint image class and corresponding classification confidence number were generated by the classification routine. The detected minutiae were classified into different categories by minutiae detection routine according to the minutiae quality number, such as >55, >65, >75, >85, or >95, representing minutiae with reliability greater than $0.55, 0.65, 0.75, 0.85,$ or 0.95, respectively. NIST software segments the whole image into blocks of 8×8 pixels and gives each block a local quality

number. The percentage of local informative blocks, i.e. blocks with non-uniform values, with local quality numbers are also calculated (zone4 representing the best and zone1 the worst). The image quality routine generates an overall quality number of the image (1, 2, 3, 4, and 5 representing best, good, average, poor and unusable, respectively). The statistical analysis was performed using the Sigma Stat software (SPSS Inc. , IL) and the data was evaluated with one-way ANOVA. All pairwise, multiple comparison were conducted with the Turkey method [22]. Statistical significance was considered when p value is less than 0.05.

A. 2D Fingerprint Analysis

To study the quantitative measures, including minutiae reliability, local image quality, overall image quality, and classification confidence number, for scanner performance evaluation, we first processed the 2D plain fingerprints with the three NIST components: PCASYS, MINDTCT and NFIQ. Figure 4 (a) illustrates the distributions of informative blocks over different local quality numbers for fingerprints with different overall image qualities. It can be seen that: 1) As the overall quality number of the fingerprints decreases from 1 (best) to 5 (unusable), the number of informative blocks with the best local quality, zone4, also decreases; 2) The numbers of informative blocks in images with overall quality number 1 and 2 are in the same order of magnitude; and 3) The number of informative blocks with the best local quality, zone4, among different overall image qualities (1$\sim$5) are significantly different (with p values less than 0.001). On the other hand, the numbers of informative blocks with less local qualities lack consistent statistical properties among different overall image qualities and cannot be used to evaluate scanner performance. Therefore, only the number of informative blocks in the best local quality zone is useful to evaluate 2D plain fingerprints.

Figure 4 (b) shows the distributions of minutiae over minutiae quality numbers greater than 0.55, 0.65, 0.75, 0.85 and 0.95 for images with different overall qualities. It can be observed that distributions of reliable minutiae in categories of $>$55, $>$65, and $>$75 have a similar pattern and each decreases as the overall quality number decreases from 1 to 4. Statistical analysis shows a significant difference for all pairwise comparisons in these three categories with the p values less than 0.01.

The number of minutiae in categories of $>$85 and $>$95 does not decease as the overall quality number decreases and also shows no statistically significant difference when compared pairwise; hence, minutiae quality numbers greater than either 0.85 or 0.95 are not reliable measures for quantifying scanner performance. The number of minutiae with reliability greater than 0.75 becomes a good measure for different overall image qualities. All the categories with less reliability (i.e. $>$55 and $>$65) show a similar pattern, $i.e.$ decreasing in minutiae number with a decrease in overall quality. Those with higher reliability ($i.e.$ $>$85 and $>$95) show no such a pattern. Moreover, Tabassi *et al* [27] have observed that, generally, a fingerprint having 20 minutiae with reliability greater than 0.75 is more likely to be identified correctly by fingerprint recognition systems. Thus, the number of minutiae with reliability greater than 0.75 can be used as another metric for the performance evaluation of 2D plain fingerprints.

Figure 4 (c) shows a scatter plot between the number of blocks with the best local quality and the number of minutiae with reliability greater than 0.75. As the number of blocks with the best local quality increases, so does the number of minutiae with reliability greater than 0.75. Jointly, these two quantities can be used to evaluate the quality of 2D plain fingerprints. Fig. 4 (d) shows the classification confidence numbers with respect to overall image quality numbers. The confidence number shows no statistically significant difference for the best, good and average quality fingerprints, but it reduces significantly as the overall quality of fingerprints further deteriorates. So, the classification confidence number, especially for the comparison between images above and below average quality, can be the fourth metric for 2D plain fingerprints evaluation.

B. 3D Fingerprint Analysis

We also studied the same set of metrics for unraveled fingerprint images generated from 3D scans. Distributions of informative blocks over local quality zones (1$\sim$4) for images with different overall qualities is illustrated in Fig. 5 (a). Although not as clear as in the 2D case, the unraveled 3D fingerprints roughly show a similar pattern among all the quality numbers. The number of informative blocks with the best local quality roughly decreases with a reduction in the overall quality of the fingerprints. It can be observed from Fig. 5 (a) that: 1) Similar to the 2D case, the number of informative blocks with local quality zone 2 also roughly increases as the overall image quality decreases; and 2)The number of informative blocks with local quality zones of 1 and 3 shows no consistent statistical properties, not useful in evaluating 3D scanner performance.

Figure 5 (b) shows the distributions of minutiae over minutiae quality numbers greater than 0.55, 0.65, 0.75, 0.85 and 0.95 for images with different overall qualities. It can be seen that the numbers of minutiae in all categories have a similar pattern: roughly decreasing as the overall image quality decreases. The number of minutiae with reliability greater than 0.75 shows a pattern similar to that observed for 2D fingerprints: significantly higher for high overall quality images than for low overall quality images. The number of minutiae with reliability greater than 0.95 does not show any statistically significant difference when compared pairwise. Therefore, as same as in the 2D case, we also chose the number of minutiae with reliability greater than 0.75 for the performance evaluation of unraveled 3D fingerprints.

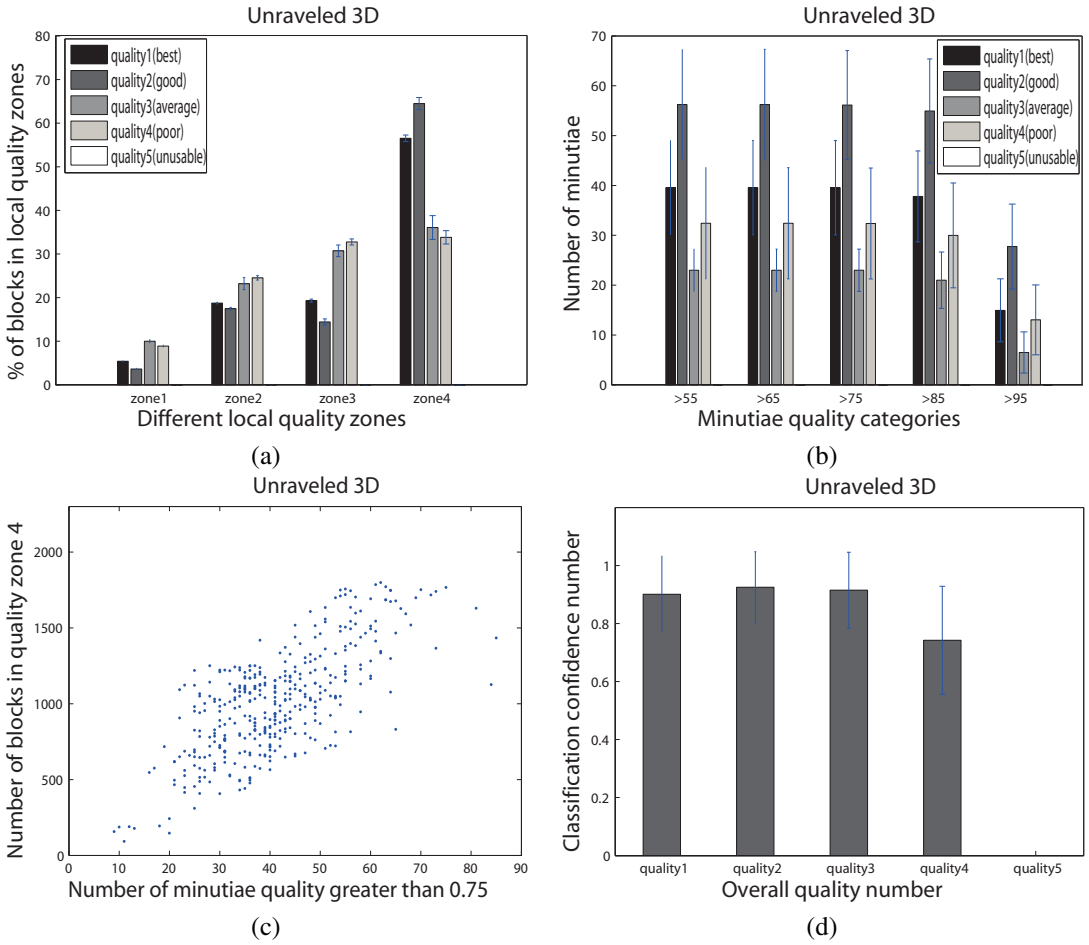

Fig. 5. Performance analysis for unraveled 3D fingerprints. Quality 1 is the best overall quality of the fingerprints. (a) Distributions of informative blocks over local quality zones (1∼4) for images with different overall qualities. Zone4 reprensets the highest local quality. (b) Distributions of minutiae over minutiae quality numbers greater than 0.55, 0.65, 0.75, 0.85 and 0.95 for unraveled 3D fingerprints with different overall image qualities. (c) Scatter plot between number of blocks in quality zone 4 and number of minutiae with quality greater than 0.75 for unraveled 3D fingerprints. (d) Plot of classification confidence numbers with respect to the overall image quality numbers for unraveled 3D fingerprints.

Figure 5 (c) shows a scatter plot between the number of informative blocks with the best local quality and the number of minutiae with reliability greater than 0.75. The former increases along with the latter, similar as in the 2D case. Moreover, the data in Fig. 5 (c) is more linearly distributed than in Fig. 4 (c), showing a stronger correlation between the two parameters. Fig. 5 (d) shows the classification confidence numbers with respect to overall image quality numbers. The confidence number is in the same order of magnitude among overall image quality numbers from 1 to 3, but significantly lower for images with the lowest overall quality, similar as in the 2D case. Thus, as in 2D plain, the contrast between the fingerprints above and below the average quality becomes useful for the performance analysis of unraveled 3D fingerprints.

The above results show that all the statistical metrics, generated by the NIST software, for traditional 2D fingerprint quality evaluation, can also be used to evaluate the quality of unraveled fingerprints obtained from the 3D scans. The scanner performance can be quantified by the scanned image quality. Higher quality of scans will lead to a superior performance of fingerprint recognition systems [23].

C. Comparison between 2D and 3D Fingerprints

Here, we compared the 2D plain fingerprints with the unraveled 3D fingerprint images using the following indexes:

1) average number of informative blocks, as well as its distribution over different local qualities (zones),
2) average number of overall qualities, as well as a sample distribution over different image qualities,
3) number of minutiae with reliability greater than 0.75, and confidence number with respect to different overall quality numbers.

The 3D scanning device produces scans larger than the 2D scans, therefore 3D scans need to be cropped before the comparison. We used 441 samples for each type of fingerprints. Fig. 6 (a) shows the average number of informative blocks for both 2D plain and unraveled 3D fingerprints. As NIST segments the whole image into blocks of 8×8 pixels, the unraveled

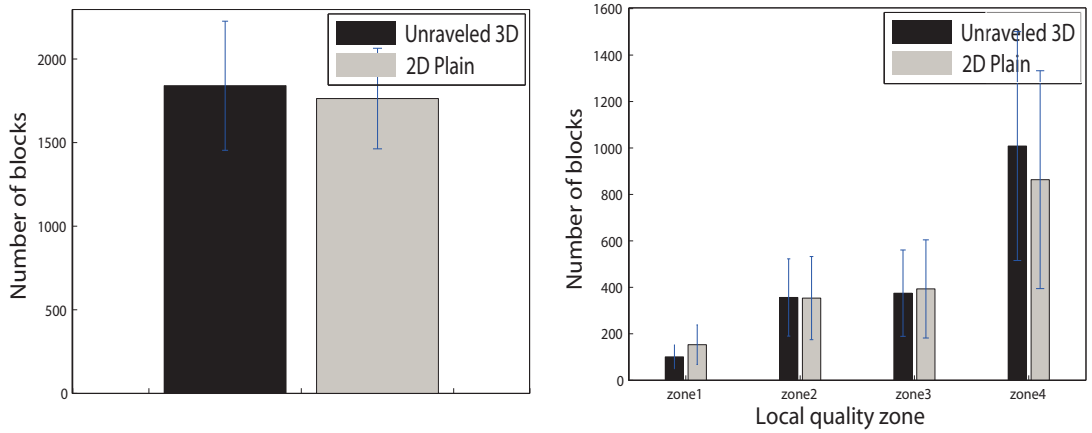

(a) (b)

Fig. 6. (a) Number of informative blocks for 2D plain fingerprints and unraveled 3D fingerprints. (b) distributions of informative blocks over different local quality zones for 2D plain fingerprints and unraveled 3D fingerprints. Zone 4 represents the best local quality.

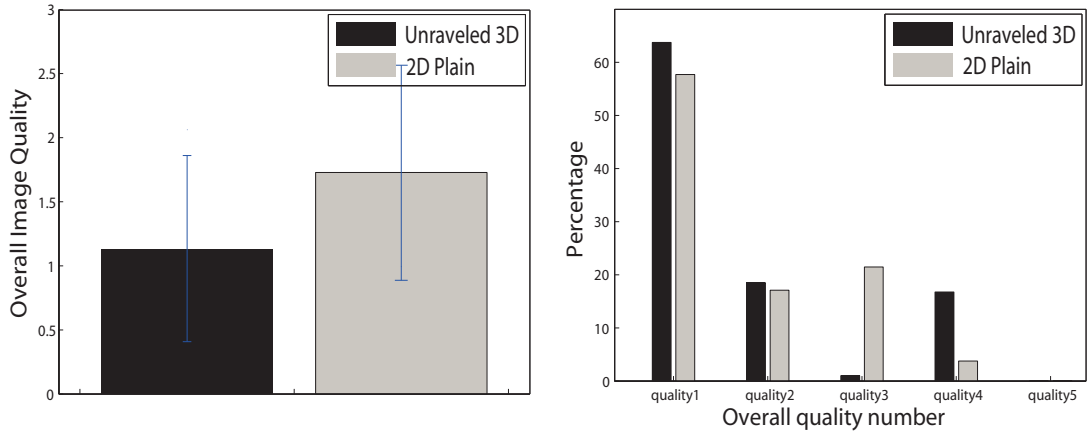

(a) (b)

Fig. 7. (a) Average of overall quality number for 2D plain fingerprints and unraveled 3D fingerprints. (b) Distributions of samples over different overall image quality numbers. Quality 1 represents the highest overall quality.

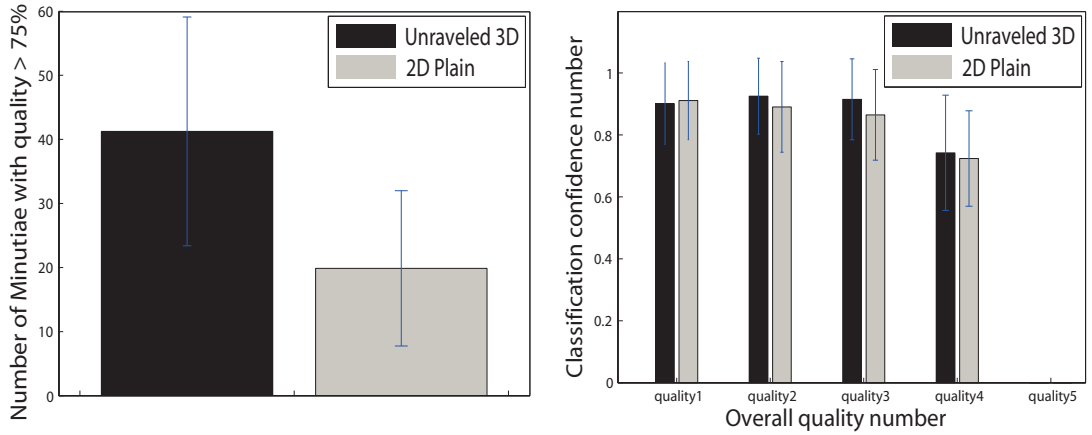

(a) (b)

Fig. 8. (a) Number of blocks for 2D plain fingerprints and unraveled 3D fingerprints. (b) Classification confidence numbers with respect to different image quality numbers.

3D fingerprints have more informative blocks than the 2D plain fingerprints in the same size. It means that with the same PPI the 3D scans contain more information than 2D scans. Further more, statistical analysis shows in Fig. 6 (b) that the unraveled 3D fingerprints have more blocks in local quality zone 4 (best) than the 2D plain fingerprints.

Figure 7 (a) shows a comparison of average image quality number between 2D and 3D samples. The average image quality of 3D fingerprints is 1.1519 and that of 2D is 1.7125. For a fair comparison in average overall quality number, the same percentage of poor quality samples were rejected from both 2D and 3D fingerprints. Fig. 7 (b) shows the distribution of image qualities of 2D and 3D samples. Although the percentages of fingerprints in quality3 and quality4 are not very stable (significant growth of 2D fingerprints from quality2 to quality3 and significant growth of 3D fingerprints from quality3 to quality4), it can be seen that the 3D fingerprints have more best quality images (63.75%) whereas 57.71 % of 2D fingerprints score the best quality number.

In the previous subsection, we observed that the quality minutiae number may not directly relate to overall image quality number. But the NIST matching software is minutiae based, and Tabassi *et al* [27] observed that generally a fingerprint containing a large number ($>$20) of minutiae with reliability higher than 0.75 was more likely to be identified correctly by the fingerprint recognition systems. Therefore, the number of minutiae with quality greater than 0.75 can be used as another important parameter for performance evaluation.

Figure 8 (a) shows the comparison between the average minutiae number with quality greater than 0.75 for 3D and 2D fingerprints. The 2D samples have 19.88 qualified minutiae on average and the 3D samples 41.25. More specifically, in terms of qualified minutiae number, the 2D fingerprints score 23.92, 21.16, 8.75 and 8.78 for overall quality number from 1 to 4; the 3D fingerprints score 39.54, 56.14, 23.00, and 32.37. The number of high quality minutiae of 3D fingerprints outperform the 2D data. Fig. 8 (b) shows distributions of the confidence number generated by the classification system over the quality number from 1 to 5 for the two data sets.

In the previous subsections, the confidence number showed no statistically significant difference for quality numbers of 1$\sim$3, but it dropped a lot for images with quality number 4. From this plot, it can be seen that although both 3D and 2D fingerprints yield almost the same confidence number for best quality images, the 3D fingerprints perform better than 2D data for lower quality images. Given the fact that the center area quality of fingerprint is what the NIST classification software concerns most, it suggests that as the overall image quality decreases, the center area quality of the 3D fingerprint does not drop as significantly as the 2D fingerprint.

VI. Conclusion

In this paper, we present a new framework for 3D fingerprint acquisition, using structured light illumination, and data processing based on 2D equivalent transform. We employed the software developed by the NIST, used for conventional 2D fingerprints, to evaluate the performance of 3D fingerprints after unraveling them into 2D equivalent ones. Compared to the 2D plain counterpart, the new non-contact 3D approach provides the superior performance in terms of the number of high quality features. Our future works include collecting a larger database, and performing the registration (authentication) on the 3D unraveled fingerprints and compare with the traditional 2D fingerprints. Further, we will employ multiple cameras and lens distortion correction [28], [29], to obtain more nail to nail information and improve ridge depth precision of 3D fingerprints. The same 3D sensor technology may be used to capture face, hand and palm-print images and therefore is ideal for a fusion of comprehensive 3D biometrics of humans.

References

[1] A. K. Jain, A. Ross, and S. Pankanti, "Biometrics: A tool for information security," *IEEE Trans. Inf. Forensics Security*, vol. 1, no. 2, pp. 125–143, Jun. 2006.

[2] S. Pankanti, S. Prabhakar, and A. K. Jain, "On the individuality of fingerprints," *IEEE Trans. Pattern Anal. Mach. Intell.*, vol. 24, no. 8, pp. 1010–1025, Aug. 2002.

[3] R. Cappelli, D. Maio, D. Maltoni, J. L. Wayman, and A. K. Jain, "Performance evaluation of fingerprint verification systems," *IEEE Trans. Pattern Anal. Mach. Intell.*, vol. 28, no. 1, pp. 3–18, Jan. 2006.

[4] R. Hashido, A. Suzuki, A. Iwata, T. Okmoto, Y. Satoh, and M. Inoue, "A capacitive fingerprint sensor chip using low-temperature poly-si TFTs on a glass substrate and a novel and unique sensing method," *IEEE J. Solid-State Circuits*, vol. 38, no. 2, pp. 274–280, Feb. 2003.

[5] N. Sato, "Novel surface structure and its fabrication process for MEMS fingerprint sensor," *IEEE Trans. Electron Devices*, vol. 52, no. 5, pp. 1026–1032, May 2005.

[6] B. Charlot, F. Parrain, N. Galy, S. Basrour, and B. Courtois, "A sweeping mode integrated fingerprint sensor with 256 tactile microbeams," *J. Microelectromech. Syst.*, vol. 13, no. 4, pp. 636–644, Aug. 2004.

[7] M. Faundez-Zanuy, "Are inkless fingerprint sensors suitable for mobile use," *IEEE Aerosp. Electron. Syst. Mag.*, vol. 19, no. 4, pp. 17–21, Apr. 2004.

[8] R. Sanchez-Reillo and L. Mengibar-Pozo, "Microprocessor smart cards with fingerprint user authentication," *IEEE Aerosp. Electron. Syst. Mag.*, vol. 18, no. 3, pp. 22–24, Mar. 2003.

[9] M. Faundez-Zanuy, "Technological evaluation of two afis systems," *IEEE Aerosp. Electron. Syst. Mag.*, vol. 20, no. 4, pp. 13–17, Apr. 2005.

[10] Wikipedia. [Online]. Available: http://en.wikipedia.org/wiki/Fingerprint

[11] N. Ratha and R. Bolle, "Automatic fingerprint recognition systems," *Sprinter-Verlag*, 2004.

[12] X. Chen, J. Tian, X. Yang, and Y. Zhang, "An algorithm for distorted fingerprint matching based on local triangle feature set," *IEEE Trans. Inf. Forensics Security*, vol. 1, no. 2, pp. 169–177, Jun. 2006.

[13] R. Rowe, S. Corcoran, K. Nixon, and R. Ostrom, "Multi-spectral imaging for biometrics," *Proc. SPIE Conf. Spectral Imaging: Instrumentation, Application, and Analysis*, pp. 90–99, Mar 2005.

[14] "Mitsubishi touchless fingerprint sensor," *http://global.mitsubishielectric.com*, Oct 2006.

[15] TBS. (2007). [Online]. Available: http://www.tbsinc.com/
[16] G. Parziale, E. Diaz-Santana, and R. Hauke, "The surround imager: A multi-camera touchless device to acquire 3d rolled-equivalent fingerprints," *On Proc. of IAPR Int. Conf. on Biometrics, LNCS*, vol. 3832, pp. 244–250, Jan 2006.
[17] V. G. Yalla and L. Hassebrook, "Very-high resolution 3d surface scanning using multi-frequency phase measuring profilometry," *Edited by Peter Tchoryk, Jr. and Brian Holz, SPIE Defense and Security, Spaceborne Sensors II, Orlando, Florida*, vol. 5798-09, pp. 44–53, 2005.
[18] J. Li, L. G. Hassebrook, and C. Guan, "Optimized two-frequency phase measuring profilometry light-sensor temporal-noise sensitivity," *J. Opt. Soc. Am. A*, vol. 20, no. 1, pp. 106–115, Jan. 2003.
[19] V. Yalla and L. G. Hassebrook, "Very-high resolution 3d surface scanning using multi-frequency phase measuring profilometry," *Spaceborne sensors II, SPIE's defense and security symposium 2005*, vol. 5798-09, pp. 1234–1240, 2005.
[20] V. Srinivasan, H. Liu, and M. Halioua, "Automated phase-measuring profilometry of 3d diffuse objects," *Applied Optics*, vol. 23, no. 18, pp. 3105–3108, 1984.
[21] J. Salvi, J. Pages, and J. Batlle, "Pattern codification strategies in structured light system," *Pattern Recognit.*, vol. 37, no. 4, pp. 827–849, Apr. 2004.
[22] A. Fatephuria, "Performance evaluation of non-contact 3-d fingerprint scanner," *Master Thesis, University of Kentucky*, Dec 2006.
[23] Y. Wang, "Performance analysis of 3-d fingerprint scan system," *Master Thesis, University of Kentucky*, Jul 2008.
[24] A. Almansa and T. Linderberg, "Fingerprint enhancement by shape adaption of scale-space operators with automatic scale selection," *IEEE Trans. Image Process.*, vol. 9, no. 12, pp. 2027–2042, Dec. 2000.
[25] L. Hong, Y. Wan, and A. Jain, "Fingerprint image enhancement: algorithm and performance evaluation," *IEEE Trans. Pattern Anal. Mach. Intell.*, vol. 20, no. 8, pp. 777–789, Aug. 1998.
[26] X. Jiang, "On orientation and anisotropy estimation for online fingerprint authentication," *IEEE Trans. Signal Process.*, vol. 53, no. 10, pp. 4038–4039, Oct. 2005.
[27] E. Tabassi, C. L. Wilson, and C. I. Watson, "Fingerprint image quality," *NIST*, Aug. 2004.
[28] Y. Wang, K. Liu, D. L. Lau, and L. G. Hassebrook, "Multicamera phase measuring profilometry for accurate depth measurement," *SPIE, Orlando, Florida*, Apr 2007.
[29] D. Boyanapally, "Merging of fingerprint scans obtained from multiple cameras in 3d fingerprint scanner system," *Master Thesis, University of Kentucky*, Feb. 2008.